*Desalination and Water Treatment*
www.deswater.com

doi:10.5004/dwt.2019.24356

160 (2019) 57–64
August

# Water harvesting from air by MOF-801/PES porous composite membranes

Yanzi Geng[a], Shuang Hao[a], Xiaoyu Lu[a], Zhiqian Jia[a,*], Shaokui Zheng[b]

[a]*Lab for Membrane Science and Technology, College of Chemistry, Beijing Normal University, Beijing 100875, China, email: zhqjia@bnu.edu.cn (Z. Jia)*
[b]*School of Environment, Beijing Normal University, Beijing 100875, China*

Received 31 January 2019; Accepted 2 May 2019

## ABSTRACT

Water harvesting from air is an effective method for solving the shortage of fresh water on the earth. Herein, MOF-801/PES porous composite membranes were prepared for capturing water from air for the first time. The effects of membrane fabrication conditions (preparation methods, relative humidity, MOF-801 contents) and re-usability on the water uptake, as well as the adsorption kinetics, were investigated. The results show that, the membranes prepared by vapor induced phase separation method (VIPS) display higher water uptake than that by non-solvent immersion precipitation separation method (NIPS), and the water uptake positively correlates with the porosity of membranes. The water uptake of membranes reaches a plateau after about 2 h, and the evolution of water uptake rates can be divided into descending rate stage and constant rate stage. The MOF-801/PES membranes prepared under the optimized conditions (60% RH, MOF-801 content of 30%) display high water uptake (about 0.027 g $g^{-1}$ or 4.13 g $m^{-2}$) under 24% ± 2% RH (17 ± 2°C) and excellent re-usability, exhibiting great potential in water harvesting.

*Keywords:* MOF-801; Water harvesting from air; Composite membranes

## 1. Introduction

On our earth, only 2.53% of the water resources is the fresh water (groundwater, lakes, rivers and creeks), wastewater, waste and domestic sewage have caused pollution of freshwater resources, which aggravates the water problem. It is reported that about 4 billion people in many developing countries are experiencing the freshwater crisis [1].

Collection and utilization of water vapor in the air plays an important role in alleviating the water shortages, and has been paid more attention in recent years [2]. Traditional materials, such as charcoal, silica gel, zeolite, etc., display either low adsorption capacity or high energy consuming for water releasing due to the too weak or too strong interactions between water and the materials [3–5]. Therefore, scientists are striving to search novel materials with high water uptake and low desorption energy.

Metal-organic frameworks (MOFs) possess adjustable pores size, excellent thermal stability, and large surface area [6,7], and have found wide applications in gas adsorption and storage [8], adsorption [9,10], pervaporation [11,12], catalysis [13], battery [14–16], drug transportation [17–20], fluorescence sensing [21–24], nonlinear optics [25], etc. Chen et al. [26] reported that NU-1500-Cr displays an impressive water vapor uptake. Ko et al. [27] found that MIL-101-$NH_2$ are capable of forming hydrogen bonds with water, and shows excellent water absorption performance. Furukawa et al. [28] reported the water absorption properties of Zr-based MOFs, and found that MOF-801 and MOF-841 possess excellent water adsorption capacity at low humidity, steep uptake behavior, recyclability and stability. However, MOFs usually exists in the form of powders or crystals, and the MOFs/air interface area is very limited. Recently, Kim et al. [29] designed a specific water uptake device with MOF-801 as adsorbents and sunlight as energy source, in which 1.79 g of MOF-801 powder was infiltrated into a porous copper foam to create an adsorbent layer (50 by 50 by 4.1 mm, packing porosity of 0.85). Nevertheless, the copper foam is expensive and the scale-up of the water up take device is difficult.

---

*Corresponding author.

Therefore, it is necessary to load MOFs on cheap and flexible carrier for practical applications [30].

Polyethersulfone (PES) is an excellent membrane material with high glass transition temperature (up to 225°C), high resistance to heat, acid, alkali, radiation and oxidation [31]. In this paper, MOF-801/PES porous composite membranes were prepared for water harvesting from air for the first time. The as-obtained plate membranes are very thin (0.25 mm or less), which is benefit for mass-transfer and water capturing. Furthermore, the membranes can be stacked or curled in plate-and-frame or spiral modules with huge specific area (100–1000 $m^2/m^3$), favoring the scale up. The effects of membrane fabrication conditions (preparation methods, relative humidity, MOF-801 contents) and re-usability on the water uptake, as well as the adsorption kinetics, were explored.

## 2. Experimental

### 2.1. Material

N, N-Dimethylformamide (DMF), methanol, ethanol, formic acid, acetone, concentrated sulfuric acid ($H_2SO_4$, 98%) were analytical grade and provided by Beijing Chemical Factory. Fumaric acid (99%) and $ZrOCl_2 \cdot 8H_2O$ were purchased from Innochem. All of the chemicals were used without further purification unless otherwise addressed. Polyethersulfone (PES, E2010) was bought from BASF Company (German). Polypropylene (PP) micro porous membranes (Φ 50 mm, pore size of 0.20 μm) were provide by Haiyan New Oriental Plastic Technology Company, China.

### 2.2. Synthesis of MOF-801

MOF-801 was prepared according to the reported procedures [29]. Typically, 1.4561 g (12.5 mmol) of fumaric acid and 4 g (12.5 mmol) of $ZrOCl_2 \cdot 8H_2O$ were dissolved in a mixed solvent of N,N-Dimethylformamide (DMF, 50 mL) and formic aid (17.5 mL), and then the mixture was transferred to an autoclave, heated in an isothermal oven at 130°C for 6 h to give as-prepared MOF-801 as white precipitate. After cooling to room temperature, the white precipitate was filtrated, and washed with DMF and methanol, and then immersed in DMF and methanol solution for 3 d to remove unreacted fumaric acid, followed by drying at 100°C under vacuum for 2 h.

### 2.3. Preparation of MOF-801/PES membranes

PES was dissolved in DMF, and then MOF-801 nanoparticles were added, stirred for 0.5 h, and cast on a clean glass plate, and then the membranes were formed by vapor induced phase separation (VIPS) method in a sealed box with constant temperature and humidity. For comparison, non-solvent immersion precipitation separation method (NIPS) was also used for fabrication of membranes by immersing the wet membranes in DI water as coagulant bath.

### 2.4. Characterization

The morphology of MOF-801 and membranes were characterized by a field emission scanning electron microscope (FESEM, S-8010, Hitachi), and the sample was sprayed with Au before observation. XRD pattern was analyzed with monochromatized Cu Kα incident radiation (Shimadzu XRD-6000). The IR spectra were recorded on a Fourier transform infrared spectrophotometer (FTIR, Affinity-1, Shimadzu, Japan).

The porosity of membranes was measured by a dry-wet weight method. Firstly, the membranes were cut into a certain size with volume of $V_0$, dried at 100°C for 1 h, and weighed ($m_1$). Then, the dry membranes were immersed in DI water for 5 h, and weighed ($m_2$) after wiping off the water on membrane surface. The membranes porosity (ε) is calculated as,

$$\varepsilon = \frac{m_2 - m_1}{\rho_{H_2O} V_0} \times 100\% \tag{1}$$

The water uptake of membranes in the air was measured by weighting method. The membranes were dried at 100°C for 1 h and weighed ($m_1$), and then placed in the air for 12 h and weighed ($m_3$). The water uptake (ϕ) was expressed as,

$$\varphi = \frac{m_3 - m_1}{m_1} \tag{2}$$

## 3. Results and discussion

### 3.1. Preparation of MOF-801

Fumaric acid reacts with $ZrOCl_2 \cdot 8H_2O$ and generates MOF-801, which possesses three-dimensional porous framework structure with fumaric acid as linker and metal cluster $Zr_6O_4(OH)_4(\text{fumarate})_6$ as the center, containing tetrahedral and octahedral cavities with slightly different size [32]. The powder X-ray diffraction (PXRD) shows sharp diffraction patterns with space group of $pn\overline{3}$ (Fig. 1a), which is consistent with the literature [29]. Fig. 1b shows that the MOF-801 particles are cubic, about 500 nm in size. In the FTIR spectra of MOF-801 (Fig. 1c), 3398 $cm^{-1}$ is the O-H stretching vibration, and 1581 and 1400 $cm^{-1}$ are asymmetric and symmetric stretching of carboxylate [33].

To measure the water uptake kinetics of MOF-801 powder, MOF-801(0.4275 g) was dried in a vacuum oven at 100°C for 2 h, and then placed in ambient conditions (30% RH, 25°C, powder thickness of 2 mm) for water uptake. Fig. 1d shows that the water uptake increases with time and then reaches equilibrium (0.23 g $g^{-1}$) after 20 h. The frame structure of MOF-801 contains three symmetric and independent cavities, two of which possess tetrahedral shape and the other has an octahedral shape, and can capture water molecules even at low relative humidity [28,29]. Choi et al. [34] analyzed the adsorption thermodynamics of MOF-801 by calculating the structural defects with the Monte Carlo method and the first principle density functional theory, and demonstrated that the high-density defects in MOF-801 are the cause of hydrophilic adsorption behavior, and the defect degree has an important influence on the moisture absorption. The water adsorption performance depends on the spatial configuration of the defects, and water condensation in the nanopores occurs preferentially along the <110> direction.

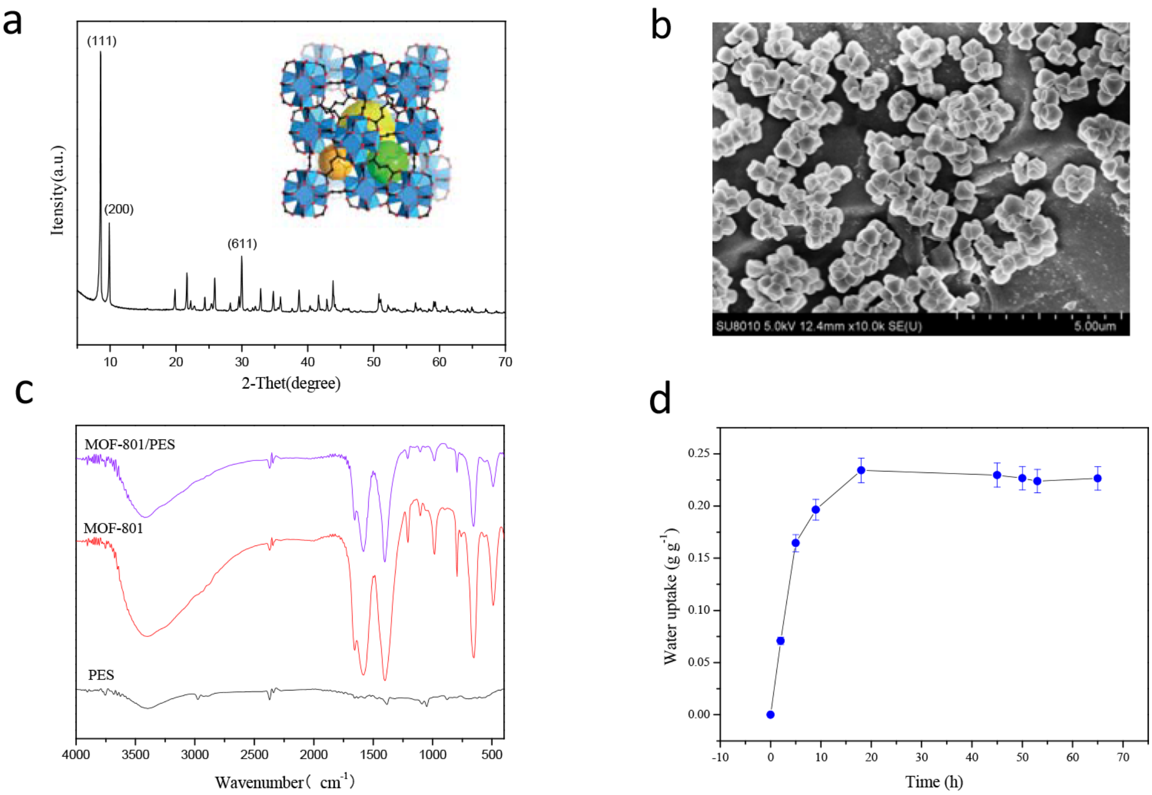

Fig. 1. Characterization of MOF-801. (a) Powered XRD patterns (The crystal structure of MOF-801 was quoted form the literature [29]). (b) SEM image. (c) FTIR spectra. (d) Water uptake kinetics of MOF-801.

### 3.2. Effects of membrane preparation methods

To explore the effects of membrane preparation methods, 15 wt % of PES solution was cast on clean glass plates, and then membrane formation was conducted by vapor induced phase separation (VIPS, 60% RH, 21°C) and immersion phase inversion (NIPS, water as coagulation bath), respectively.

In the FTIR spectra of PES membranes (Fig. 1c), the peaks at 1577 cm$^{-1}$ and 1485 cm$^{-1}$ are ascribed to C=C stretching of benzene ring. The bands at 1321 cm$^{-1}$ and 1297 cm$^{-1}$ are attributed to the asymmetric stretching of sulfone, and 1149 cm$^{-1}$ is the symmetric stretching of sulfone. 1238 cm$^{-1}$ is the asymmetric stretching vibration of C-O-C, and 1104 cm$^{-1}$ is the C-O stretching vibration. 871, 800, and 835 cm$^{-1}$ are C-H deformation vibrations of substituted benzene rings [31].

Figs. 2a and 2b show that the membrane prepared by the VIPS method possesses a honeycomb network structure with pores size about 5.92 µm, whereas the membrane prepared by the NIPS method displays smaller pores size (about 800 nm). For VIPS method, the water content in vapor is limited, and the exchange rate of water in vapor with the solvent in wet membrane is low, leading to slow phase separation and thus porous network structure [35]. In contrast, in NIPS process the wet membrane contacts directly with the water, and the exchange rate between the solvent and water is very high, resulting in sponge-like membrane with small pores.

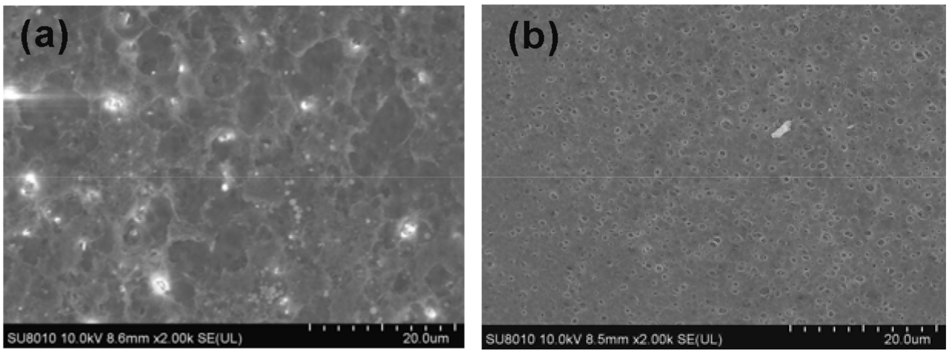

Fig. 2. Effects of preparation methods on PES membranes. (a) Membranes prepared by VIPS. (b) Membranes prepared by NIPS.

The water uptake of PES membranes (thickness of 0.25 mm) were measured at ambient conditions (30% RH and 22°C in average) for 12 h. The membrane prepared by VIPS method displays higher water uptake (0.0060 g $g^{-1}$ or 0.34 g $m^{-2}$) than that by the NIPS method (0.0045 g $g^{-1}$ or 0.28 g $m^{-2}$). It can be seen that the membrane structure has an important influence on the water uptake [36]. Hereafter, VIPS method was used for preparation of membranes.

### 3.3. Effect of relative humidity on membrane formation

To investigate the effects of relative humidity on the membrane formation, 15 wt% PES solution was cast on glass plate and then placed in a constant humidity and temperature environment (20% RH, 40% RH, 60% RH, 80% RH, 25°C) respectively for 10 h.

Fig. 3 shows the SEM image of membranes. The membrane prepared at 20% RH exhibits dense structure. In this case, the water content in vapor is small, and the driving force for water entering into the wet membrane is low, and solvent evaporation is the main mechanism for membrane formation [35]. The membrane obtained at 40% RH possesses many small pores (about 450 nm in size) on the surface. For the membrane prepared at 60% RH, the pores number increases because the diffusion rate of water vapor to the wet membrane rises [37–39]. The membrane fabricated at 80% RH displays large and wide-distributed pores size (2.14–9.28 μm) due to the too fast membrane formation rate.

Fig. 4a shows that, with the increased relative humidity in membrane preparation, the membrane porosity and water uptake (in the air of 23 ± 2% RH and 15 ± 2°C in average for 12 h) rise firstly and then decline, and the uptake positively correlates with the porosity. The membrane prepared at 60% RH displays the highest porosity (5.53%) and water uptake (0.0036 g $g^{-1}$). Therefore, 60% RH was used for membrane fabrication in the subsequent experiments.

### 3.4. Effects of MOF-801 contents

To investigate the effects of MOF-801 contents, the casting solution of MOF-801/PES (total solid content of 15 wt %, in which MOF-801 accounting for 0, 10, 20, 30, 40, and 50% of the total solid content) was cast on glass plate, and the membranes formation was carried out at 60% RH (25°C). The FTIR spectra of MOF-801/PES membranes (Fig.1c) show that the feature peaks of PES and MOF-801 appear.

Fig. 5 shows the SEM images of membranes. When the MOF-801content is 30% or less, some MOF-801 particles can be seen in the membrane surface layer. For MOF-801 content of 40% and 50%, lots of MOF-801 aggregates are observed on the membrane surface, and the membrane becomes brittle. Furthermore, with the rising MOF-801 contents, the porosity and water uptake (in the air of 21 ± 2%RH and 15 ± 2°C in average for 12 h) of membranes increase (Fig. 4b). For 30% of MOF-801, the porosity is 18.66% and the water uptake attains 0.0125g $g^{-1}$ (i.e. 1.69 g $m^{-2}$). Considering the membranes stability, MOF-801 content of 30% was employed as the optimized condition.

### 3.5. Adsorption kinetics

To explore the adsorption kinetics of membranes, the evolution of water uptake with time was measured for

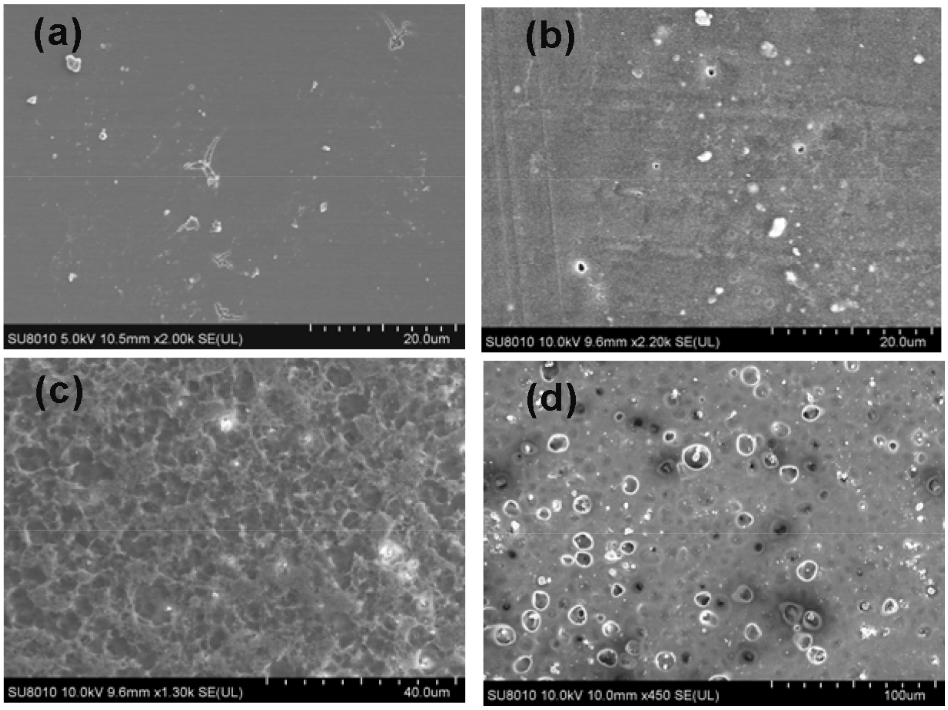

Fig. 3. Effects of relative humidity on PES membranes. (a) 20% RH, (b) 40% RH, (c) 60% RH, and (d) 80% RH.

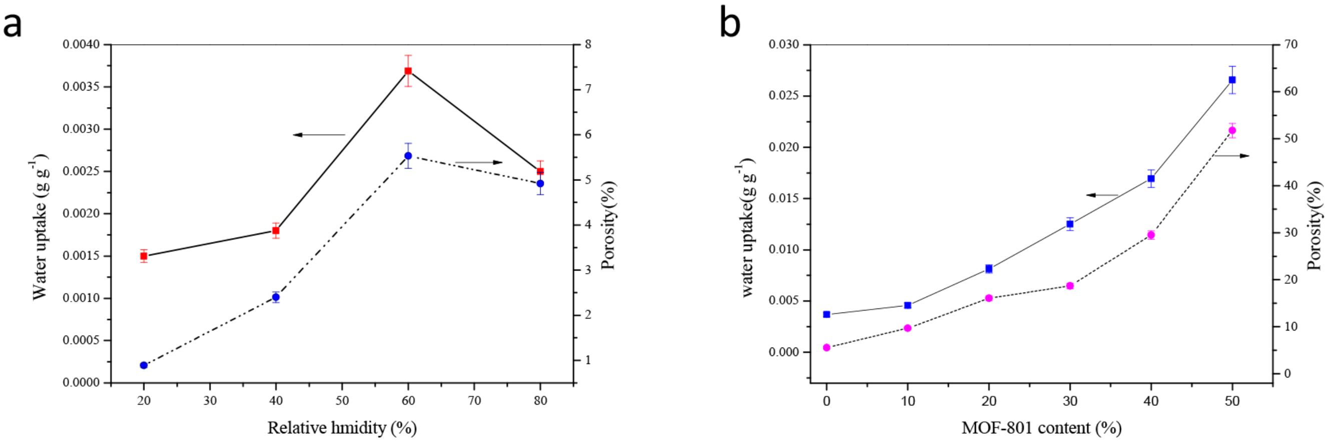

Fig. 4. (a) Effect of relative humidity in membrane preparation on water uptake of PES membrane. (b) Effect of MOF-801 contents on water uptake of MOF-801/PES membrane.

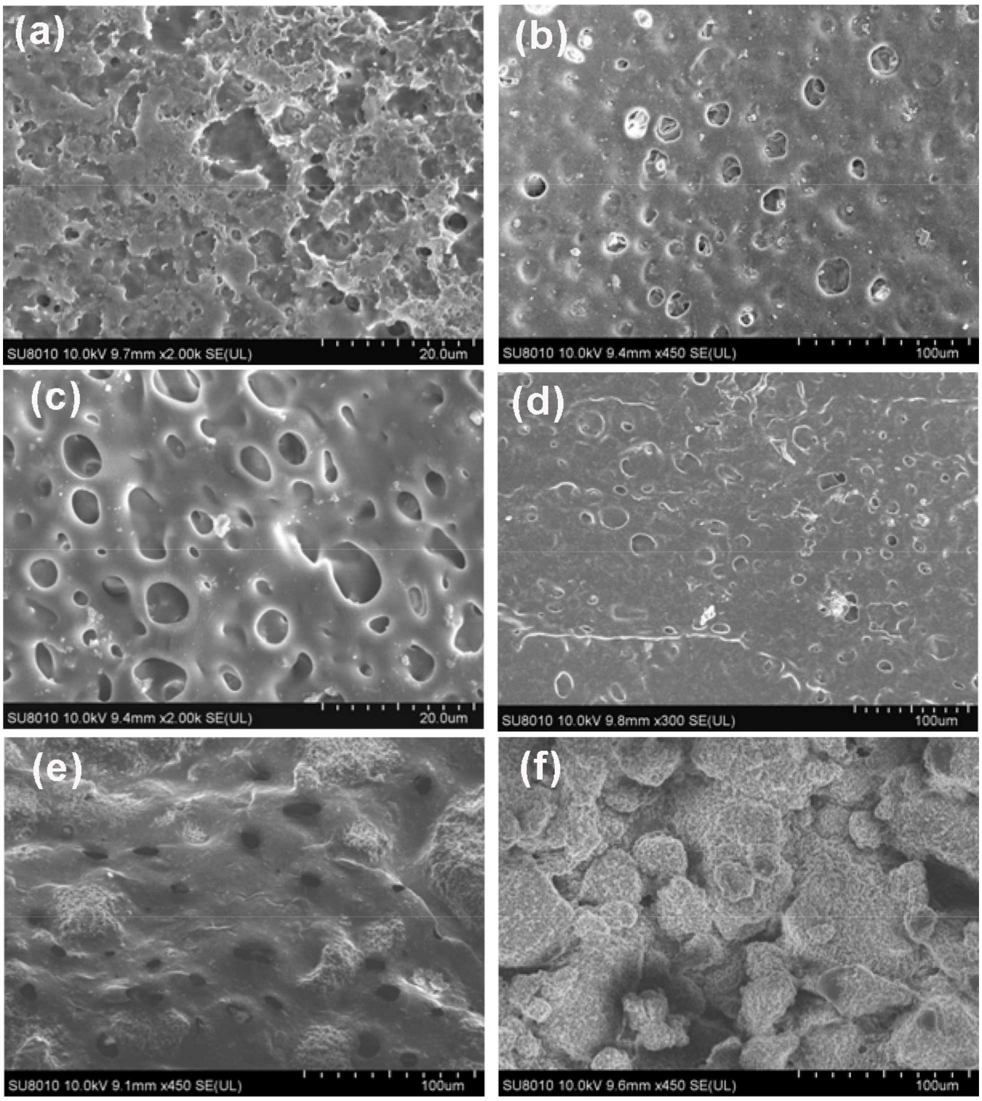

Fig. 5. Effect of MOF-801 contents on membranes. (a) 0% of MOF-801. (b) 10% of MOF-801. (c) 20% of MOF-801. (d) 30% of MOF-801. (e) 40% of MOF-801. (f) 50% of MOF-801.

MOF-801/PES composite membranes (MOF-801 content of 0%, 30%, 40%, and 50% respectively) under ambient conditions (27% RH and 18°C in average). The water uptake increases with time gradually and reaches a plateau after 2 h (Fig. 6a). The average water uptake of membranes with MOF-801 content of 50%, 40% and 30% is about 5.78, 4.49 and 2.47 times that of the pristine PES membrane, demonstrating that MOF-801 mainly contributes to the uptake of membranes.

Fig. 6b displays the change of water uptake rates with time. The evolution of water uptake rates can be divided into two stages: descending rate stage, and constant rate stage. In water capturing, the temperature and humidity of the air can be considered as constant, and the water uptake rate can be expressed as,

$$N_A = k_H \left( H - H_W \right) \tag{3}$$

where $N_A$ is the water uptake rate, $k_H$ is the mass transfer coefficient which can be regarded as constant in a certain condition, $H$ is the air humidity, and $H_W$ the equilibrium humidity on the membranes surface. In the initial stage, the membranes are dry, and $H_W$ is very low and the driving force for mass transfer is high, resulting in large uptake rate. For MOF-801 content of 0%, 30%, 40%, and 50%, the initial mass transfer coefficient is found to be about 1.99, 1.33, 3.65 and 3.76 g h$^{-1}$ m$^{-2}$ respectively. With the proceeding of water uptake, $H_W$ increases, and the water adsorption sites change from the membrane surface to the membrane interior, and from large pores of membranes to small pores, leading to declined uptake rates. When the membranes are saturated with water, $H_W$ and uptake rate become almost constant, displaying a constant rate stage.

### 3.6. Membranes re-usability

To investigate the re-usability of membranes (MOF-801 contents of 0%, 10% and 30%), water harvesting was conducted in the air (24% ± 2% RH, 17 ± 2°C), and then water releasing was carried out by heating (100°C) to simulate the solar thermal heating (Fig. 7). The membranes were reused for four water harvesting/water releasing cycles. Fig. 8 shows that there is not obvious change in water uptake of MOF-801/PES composite membranes (about 0.027 g g$^{-1}$, or 4.13 g m$^{-2}$) in the four cycles, demonstrating excellent stability and re-usability of the membranes.

The comparison with other materials for water capturing reported in literature was given in Table 1. It can be seen that the MOF-801/PES composite membranes showed higher water-uptake capacity than PIZOF-2, or comparable capacity with Cr-MOF-1. More importantly, the MOF-801/PES composite membranes can be easily scaled up. In practical applications, the plate MOF-801/

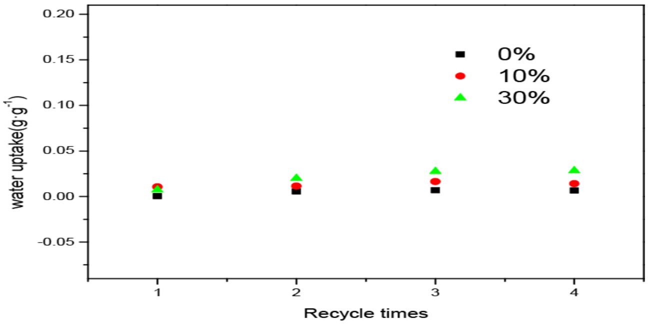

Fig. 8. Re-usability of membranes.

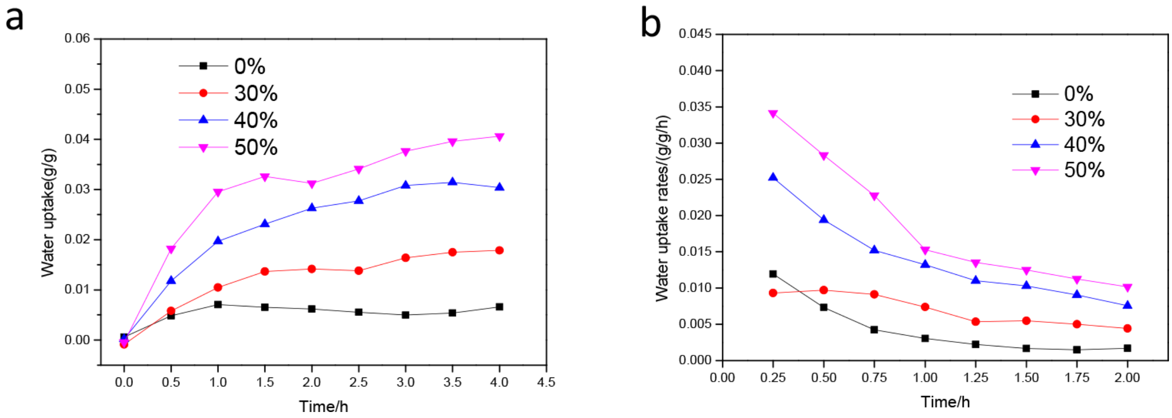

Fig. 6. Adsorption kinetics MOF-801/PES composite membranes. (a) Evolution of water uptake. (b) Evolution of water uptake rates.

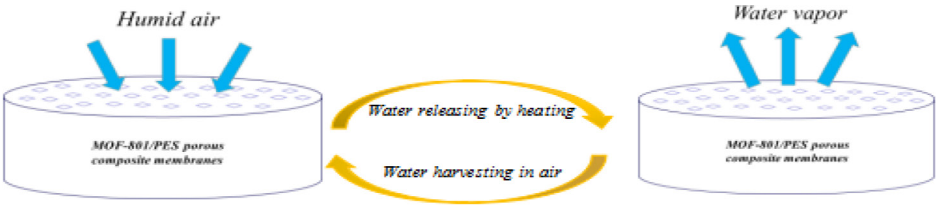

Fig. 7. Schematic of water harvesting/water releasing cycles.

Table 1
Comparison with other materials for water capturing

| Adsorpbent | Water uptake (20%–40%RH) (g/g) | Reference |
|---|---|---|
| Cr-MOF-1 | 0.03 | [26] |
| NU-1500-Cr | 0.06 | [26] |
| PIZOF-2 | 0.01 | [28] |
| UiO-66 | 0.09 | [28] |
| MIL-101-Cr | 0.11 | [27] |
| MIL-101-Cr | 0.14 | [27] |
| MOF-801/PES | 0.027 | This study |

PES membranes can be curled into spiral modules with specific area of about 500 $m^2/m^3$. The adsorption of water can be conducted during cool night, and release can be carried out by sunlight heating during the warm day, and water harvest can be achieved by a condenser. In term of the water harvesting/water releasing data of MOF-801/PES composite membranes (about 4.13 g $m^{-2}$) in this study, 1.5 L of water is expected to be obtained per day per $m^3$ without additional energy input. The practical water harvesting/releasing experiments are now being studied in our Lab.

## 4. Conclusions

MOF-801/PES composite membranes were prepared for water harvesting from air for the first time. The water uptake of membranes reaches a plateau after about 6 h, and the evolution of water uptake rates can be divided into descending rate stage and constant rate stage. The water-uptake capacity positively correlates with the porosity of membranes. Under the optimized membrane formation conditions (60% RH, MOF-801 content of 30%), the membranes displays high water uptake (about 0.027 g $g^{-1}$, or 4.13 g $m^{-2}$) under 24% ± 2% RH (17 ± 2°C) and excellent re-usability, demonstrating great potential in water harvesting from air.

## Acknowledgments

This work was supported by the National Natural Science Foundation of China and Qinghai Qaidam Saline Lake Chemical Science Research Joint Fund (No. U1607109).

## References

[1] M.M. Mekonnen, A.Y. Hoekstra, Four billion people facing severe water scarcity, Sci Adv., 2 (2016) e1500323.

[2] D. Noone, J. Galewsky, Z.D. Sharp, J. Worden, J. Barnes, D. Baer, A. Bailey, D.P. Brown, L. Christensen, E. Crosson, F. Dong, J.V. Hurley, L.R. Johnson, M. Strong, D. Toohey, A. Van Pelt, J.S. Wright, Properties of air mass mixing and humidity in the subtropics from measurements of the D/H isotope ratio of water vapor at the Mauna Loa Observatory, J. Geophys. Res. Atmospheres, 116 (2011) n/a-n/a.

[3] J. Canivet, A. Fateeva, Y. Guo, B. Coasne, D. Farrusseng, Water adsorption in MOFs: fundamentals and applications, Chem. Soc. Rev., 43 (2014) 5594–5617.

[4] N.C. Burtch, H. Jasuja, K.S. Walton, Water stability and adsorption in metal-organic frameworks, Chem. Rev., 114 (2014) 10575–10612.

[5] C. Wang, X. Liu, D.N. Keser, J.P. Chen, K. Li, Applications of water stable metal-organic frameworks, Chem. Soc. Rev., 45 (2016) 5107.

[6] R. Saidur, S.N. Kazi, M.S. Hossain, M.M. Rahman, H.A. Mohammed, A review on the performance of nanoparticles suspended with refrigerants and lubricating oils in refrigeration systems, Renew. Sust. Energ. Rev., 15 (2011) 310–323.

[7] M.S. Gruszkiewicz, J.M. Simonson, T.D. Burchell, D.R. Cole, Water adsorption and desorption on micro porous solids at elevated temperature, J. Thermal. Anal. Calorim., 81 (2005) 609–615.

[8] Y.L. And, R.T. Yang, Gas adsorption and storage in metal-organic framework MOF-177, Langmuir ACS J. Surfaces Colloids, 23 (2007) 12937.

[9] Y. Guo, Z. Jia, Novel sandwich structure adsorptive membranes for removal of 4-nitrotoluene from water, J. Hazard. Mater., 317 (2016) 295–302.

[10] Z. Jia, M. Jiang, G. Wu, Amino-MIL-53(Al) Sandwich-structure membranes for adsorption of p-nitrophenol from aqueous solutions, Chem. Eng. J., 307 (2017) 283–290.

[11] Z. Jia, G. Wu, Metal-organic frameworks based mixed matrix membranes for pervaporation, Micropor. Mesopor. Mater., 235 (2016) 151–159.

[12] G. Wu, M. Jiang, T. Zhang, Z. Jia, Tunable pervaporation performance of modified MIL-53(Al)-NH 2 /poly(vinyl alcohol) mixed matrix membranes, J. Membr. Sci., 507 (2016) 72–80.

[13] M. Sabo, A. Henschel, H. Fröde, E. Klemm, S. Kaskel, Solution infiltration of palladium into MOF-5: Synthesis, physisorption and catalytic properties, J. Mater. Chem., 17 (2007) 3827–3832.

[14] S. Maiti, T. Dhawa, A.K. Mallik, S. Mahanty, $CeO_2$@C derived from benzene carboxylate bridged metal-organic frameworks: ligand induced morphology evolution and influence on the electrochemical properties as a lithium-ion battery anode, Sustain. Energ. Fuels, 1 (2017) 288–298.

[15] H. Park, D.J. Siegel, Tuning the adsorption of polysulfides in lithium–sulfur batteries with metal-organic frameworks, Chem. Mater., 29 (2017) 4932–4939.

[16] G. Huang, D. Yin, F. Zhang, Q. Li, L. Wang, Yolk@shell or concave cubic NiO–$Co_3O_4$@C nanocomposites derived from metal-organic frameworks for advanced lithium-ion battery anodes, Inorg Chem., 56 (2017) 9794–9801.

[17] X. Kuang, Y. Ma, H. Su, J. Zhang, Y. Dong, B. Tang, High-performance liquid chromatographic enantioseparation of racemic drugs based on homochiral metal-organic framework, Anal. Chem., 86 (2014) 1277–1281.

[18] J. Gordon, H. Kazemian, S. Rohani, MIL-53(Fe), MIL-101, and SBA-15 porous materials: Potential platforms for drug delivery, Mater. Sci. Eng. C, 47 (2015) 172–179.

[19] D. Cunha, M.B. Yahia, S. Hall, S.R. Miller, H. Chevreau, E. Elkaïm, G. Maurin, P. Horcajada, C. Serre, Rationale of drug encapsulation and release from biocompatible porous metal-organic frameworks, Chem. Mater., 25 (2013) 2767–2776.

[20] P. Davydovskaya, R. Pohle, A. Tawil, M. Fleischer, Work function based gas sensing with Cu-BTC metal-organic framework for selective aldehyde detection, Sensors Actuators B: Chem., 187 (2013) 142–146.

[21] V. Pentyala, P. Davydovskaya, M. Ade, R. Pohle, G. Urban, Metal-organic frameworks for alcohol gas sensor, Sensors Actuators B: Chem., 222 (2016) 904–909.

[22] J. Hromadka, B. Tokay, S. James, R.P. Tatam, S. Korposh, Optical fibre long period grating gas sensor modified with metal organic framework thin films, Sensors Actuators B: Chem., 221 (2015) 891–899.

[23] S. Ohira, Y. Miki, T. Matsuzaki, N. Nakamura, Y. Sato, Y. Hirose, K. Toda, A fiber optic sensor with a metal organic framework as a sensing material for trace levels of water in industrial gases, Anal. Chim. Acta., 886 (2015) 188–193.

[24] X. Wan, H. Song, D. Zhao, L. Zhang, Y. Lv, A Y-doped metal-organic framework-based cataluminescence gas sensor for isobutanol, Sensors Actuators B: Chem., 201 (2014) 413–419.

[25] L.N. Duan, Q.Q. Dang, C.Y. Han, X.M. Zhang, An inter penetrated bioactive nonlinear optical MOF containing a coordinated quinolone-like drug and Zn(II) for pH-responsive release, Dalton Trans., 44 (2015) 1800.

[26] Z. Chen, P. Li, X. Zhang, P. Li, M.C. Wasson, T. Islamoglu, J.F. Stoddart, O.K. Farha, Reticular access to highly porous ACS-MOFs with rigid trigonal prismatic linkers for water sorption, J. Am. Chem. Soc., 141 (2019) 2900–2905.

[27] A.P.G.C. Nakeun Ko, Tailoring the water adsorption properties of MIL-101 metal-organic frameworks by partial functionalization, J. Mater. Chem. A., (2015).

[28] H. Furukawa, F. Gándara, Y. Zhang, J. Jiang, W.L. Queen, M.R. Hudson, O.M. Yaghi, Water adsorption in porous metal-organic frameworks and related materials, J. Am. Chem. Soc., 136 (2014) 4369–4381.

[29] H. Kim, S. Yang, S.R. Rao, S. Narayanan, E.A. Kapustin, H. Furukawa, A.S. Umans, O.M. Yaghi, E.N. Wang, Water harvesting from air with metal-organic frameworks powered by natural sunlight, Science, 358 (2017) 430.

[30] M.J. Kalmutzki, C.S. Diercks, O.M. Yaghi, Metal-organic frameworks for water harvesting from air, Adv. Mater., 30 (2018) 1704304.

[31] I. Sadeghi, A. Aroujalian, A. Raisi, B. Dabir, M. Fathizadeh, Surface modification of polyethersulfone ultrafiltration membranes by corona air plasma for separation of oil/water emulsion, J. Membr. Sci., 430 (2013) 24–36.

[32] S.A. Jovial, Crystals Growth Study of Micro porous Metal-Organic Frameworks by Atomic Force Microscopy. 2015.

[33] X. Zhu, C. Yang, X. Yan, Metal-organic framework-801 for efficient removal of fluoride from water, Micropor. Mesopor. Mater., 259 (2018) 163–170.

[34] J. Choi, L. Lin, J.C. Grossman, Role of structural defects in the water adsorption properties of MOF-801, J. Phys. Chem. C., 122 (2018) 5545–5552.

[35] Y.L. Peng, H.W. Fan, Y.N. Song, Research on the process of membrane formation via water-vapor induced phase separation, J. Beijing Univ. Technol., 38 (2012) 1418–1423.

[36] J.T. Tsai, Y.S. Su, D.M. Wang, J.L. Kuo, J.Y. Lai, A. Deratani, Retainment of pore connectivity in membranes prepared with vapor-induced phase separation, J. Membr. Sci., 362 (2010) 360–373.

[37] D. Bouyer, W. Werapun, C. Pochat-Bohatier, A. Deratani, Morphological properties of membranes fabricated by VIPS process using PEI/NMP/water system: SEM analysis and mass transfer modelling, J. Membr. Sci., 349 (2010) 97–112.

[38] C. Li, D. Wang, A. Deratani, D. Quémener, D. Bouyer, J. Lai, Insight into the preparation of poly(vinylidene fluoride) membranes by vapor-induced phase separation, J. Membr. Sci., 361 (2010) 154–166.

[39] P. Menut, Y.S. Su, W. Chinpa, C. Pochat-Bohatier, A. Deratani, D.M. Wang, P. Huguet, C.Y. Kuo, J.Y. Lai, C. Dupuy, A top surface liquid layer during membrane formation using vapor-induced phase separation(VIPS)-Evidence and mechanism of formation, J. Membr. Sci., 310 (2008) 278–288.